ICANS XIX,
19th meeting on Collaboration of Advanced Neutron Sources
March 8 – 12, 2010
Grindelwald, Switzerland

DEVELOPMENT OF A BEAM-LINE FOR SPIN ECHO SCATTERING ANGLE MEASUREMENT AT THE LOW ENERGY NEUTRON SOURCE

A. L. WASHINGTON
Center for the Exploration of Energy and Matter, Indiana University, 2401 Milo Sampson Lane, Bloomington, IN 47408, USA

and

P. STONAHA, RANA ASHKAR, AND ROGER PYNN
Center for the Exploration of Energy and Matter, Indiana University, 2401 Milo Sampson Lane, Bloomington, IN 47405-7105, USA
V. R. SHAH
Nebraska Center for Materials and Nanoscience, University of Nebraska, Lincoln, NE, 68588-0113, USA

ABSTRACT
A polarized neutron beam line has been installed at the Center for the Exploration of Energy and Matter (CEEM) as part of the Low Energy Neutron Source (LENS) project. Principally, the beam line is designed to support development of SESAME (Spin Echo Scattering Angle Measurement) and other polarized neutron instrumentation. The beam-line uses inclinable optic benches, which makes it useful for transmission and reflection measurements on both solid and liquid samples. SESAME uses triangular cross-section solenoids that can be reproducibly mounted and removed from the optic benches. The incident polarized beam is established using a compact neutron bender-polarizer mounted between two supermirror guides inclined to one another by 1.5°. The polarization of the scattered beam is analyzed with a wide-angle array of transmission supermirrors oriented radially from the sample. The scattered neutron beam is detected by a scintillating detector with ~0.5 mm position sensitivity over an active area of 20 x 20 cm^2.

1. Introduction

Liouville's theorem has always been a limiting factor in neutron scattering measurements. Any attempt to focus the neutron beam onto the sample will result in increased beam divergence and decreased momentum resolution. In traditional neutron scattering experiments, the only way to achieve good resolution has been to cut down the phase space and lose neutron flux. To escape this limitation, the Spin Echo Scattering Angle Measurement (SESAME) technique encodes the scattering angle in the neutron's polarization [1]. This eliminates, to a large extent, the coupling between beam collimation and momentum resolution, allowing for measurements of large scattering objects without unacceptable losses of neutron flux.

The SESAME technique uses a polarized incident neutron beam. The beam first passes through an abrupt, 90˚ change in the magnetic field direction, which splits the neutron beam into two in-phase wave states with opposite spins $|+z\rangle$ and $|-z\rangle$, as shown in Figure 1. These wave states then propagate through triangular shaped magnetic field regions with magnetic fields alternately along the plus- and minus-z directions. Since the

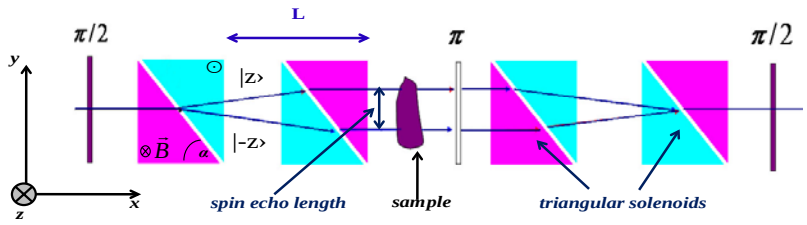

Figure 1: Schematic of the SESAME instrument. The alternating shades in the triangles represent the alternating field directions in the solenoids.

total energy of each neutron is conserved, the neutron's speed depends on its Zeeman interaction with the surrounding magnetic field, and the two spin states refract in different directions when they pass through the inclined boundary between the triangular regions. A second pair of triangles, with opposite fields to the first, returns the neutron waves to being parallel, yet spatially separated by a distance of the order of a few hundred nanometers, known as the spin echo length. The secondary spectrometer recombines the two neutron spin states, leading to spin echo. Any scattering from a sample will result in a relative phase between the two wave states at the end of the instrument, and the initial polarization will not be retrieved: i.e. the echo polarization will be diminished. The polarization of the outgoing neutron beam is linearly proportional to the cosine of the scattering angle, allowing SESAME to measure scattering via the final beam polarization.

2. Instrument Description

2.1 Neutron Optics

Neutrons are transported to the SESAME instrument at LENS by two segments of rectangular cross-section neutron guides (25mm tall x 75mm wide) which make an angle of 1.5° with one another in the vertical plane. The sides of the neutron guides are coated with Ni/Ti supermirrors whose critical angle is 3 times that of Ni (i.e. m=3 coating), while the top and bottom are coated with m=2 supermirrors of the same material. A solid-state polarizing bender is used to transport neutrons through the break between the guides. The bender serves a dual purpose: 1) The incident beam emerges polarized, albeit with an intensity loss of more than 50%, and 2) fast neutrons cannot propagate through the guide system along any straight line path. The bender consists of a stack of 170 curved silicon wafers 150 μm thick. On the convex side of each wafer is an m=3 polarizing supermirror composed of layers of $Fe_{89}Co_{11}$ and Si, followed by a Gd/Si antireflecting layers and then an absorbing layer of Gd. On the other side is an m=2 polarizing supermirror composed of layers of Fe and Si and the same antireflecting and absorbing layers. The goal is to reflect the desired spin state into the second guide with the other spin state absorbed in the gadolinium. The bender and one guide segment are both mounted on a concrete beam shutter, so that they are removed from the beamline when the shutter is raised hydraulically to block the neutron beam. When the shutter is lowered it comes to rest on a kinematic mount that ensures correct reproducible alignment of the guide and bender. The neutron transmission of the bender is given in Figure 2. We are still investigating the discrepancy between the expected and measured transmission.

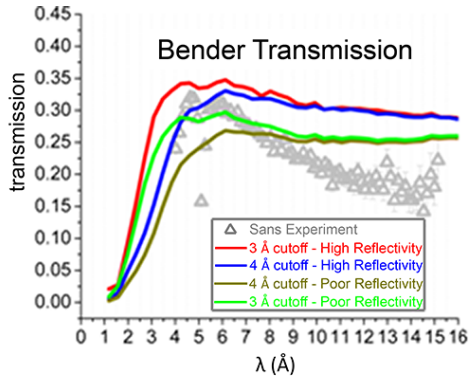

Figure 2: VITESS simulations with different cut-off wavelengths and supermirror reflectivities.

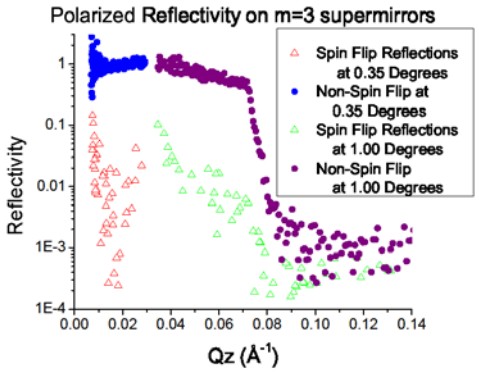

Figure 3: Polarized neutron reflectivity for the walls of the Ni/Ti-coated neutron guide[1]. A 300G field was applied perpendicular to the guide wall.

The neutron guide segment after the bender is magnetized with a ~300 Gauss magnetic field by means of ceramic magnets in order to preserve the neutron polarization created by the bender. This field is perpendicular to the beam direction and to the side walls of the guide. We have verified (Figure 3) that in this geometry there is less than ~2% depolarization of neutrons reflected from the side walls of the guide.

The profile of the beam is defined by two sets of motorized slits purchased from Advanced Design Consulting USA, Inc [2]. Each set of slits contains four boron carbide blades, allowing horizontal and vertical control of the beam size with 3 μm precision. The slits provide a maximum beam aperture of 60 mm × 60 mm. Both sets of slits can be positioned anywhere along the flight path on optic rail.

A wide-angle transmission polarization analyzer measures the polarization of the scattered neutron beam. The analyzer consists of eighteen 0.7 mm-thick glass plates that radiate from a point 1750 mm upstream of the analyzer. Each plate is coated with Gd_2O_3 to absorb neutrons. There is an angle of 0.2235˚ between neighboring glass plates, giving a total acceptance of 2° above and below the direct beam. Polarizing m=2.3 supermirrors are located between neighboring glass plates at an angle of 0.95˚ to the central path between these plates. The supermirrors reflect one spin state into the Gd_2O_3-coated glass and transmit the remaining neutrons to the detector. Ceramic magnets outside of the analyzer magnetize the supermirrors with a field of 0.12 T. A schematic layout of the instrument is shown in Figure 4.

2.2 Larmor Devices

The SESAME instrument requires four pairs of triangular solenoids to refract the spin states of the neutron beam. The solenoids are wrapped with an aluminum wire coated in an enamel of oxide from which water was removed by a baking process. The wires are wrapped around a right triangular aluminum frame (Figure 5) with sides measuring 10.1 cm in the x-direction, 6.9 cm in the y-direction and 14.0 cm in the z direction. Through the center of the aluminum frame a rectangular hole is bored out along the x-direction, spanning 4 cm in the y-direction and 7 cm in the z-direction. To eliminate return fields in the neutron beam line, each pair of solenoids is yoked in 1/16”-thick mumetal. To allow spin transport through the instrument and to remove as much aluminum as possible from

[1] Due to poor statistics at long wavelengths, the data at the lowest values of Q recorded at each reflection angle in Figure 3 are unreliable.

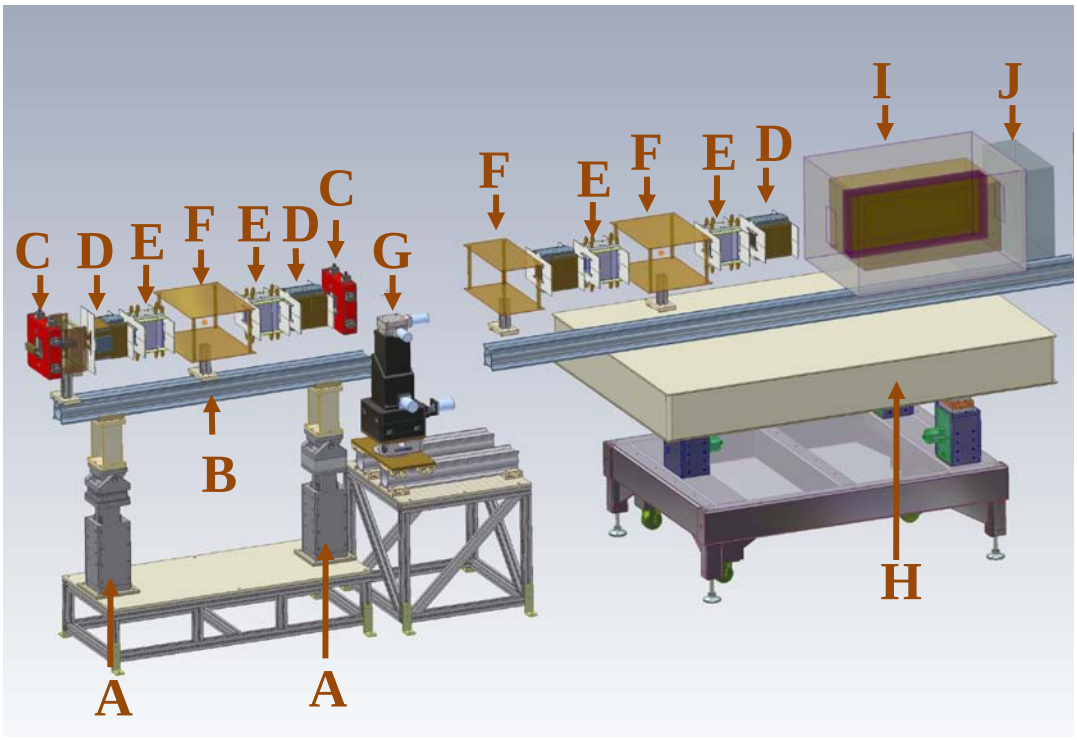

Figure 4: Schematic Layout of SESAME instrument. Major beam-line components have been labeled: A - Jacks to tilt the incident beamline; B – Upstream optic rail; C – Slits; D – Flippers; E - Triangular Solenoid Pairs; F – Guide Fields; G – Sample Goniometer; H – Tiltable Optic Table; I –Polarization Analyzer; J – Detector

the neutron beam, each triangle has a 6.0 cm tall x 8.0 cm wide gap in the winding of the leading face through which the neutron beam passes. This gap is produced during the winding process by adding a piece of custom-machined aluminum into the center hole of the triangular frame. The shape of this piece was designed so that each turn of wire in the gap region could be folded against the face of the coil, as seen in Figure 6. Experiments at the NCNR (Figure 7) verified that the integral of the field modulus along a neutron path depends linearly on the distance (y) of the neutron trajectory from the neutron beam center. The fields within the triangular solenoids were mapped both within and outside of a solenoid and compared to numerical calculations based on an infinite solenoid plus a current sheet at the location of the gap. The mapped fields (Figure 8) agreed with the calculations to within 2%.

Each triangle coil is individually powered by a Kepco BOP 20-20M bipolar power supply operating in constant current mode. The output current is controlled via a computer through a National Instruments DAC card. Each coil has a resistance of 1.1 Ohms. Field mapping has shown that the magnets produce 8.85 Gauss per Ampere at the hypotenuse of the triangular cross section.

To prevent the solenoids from overheating, each triangular frame is water-cooled through three 3/8” diameter holes parallel to the magnetic field generated by the solenoid. Thermal imaging has shown that the increase in water temperature after passing through

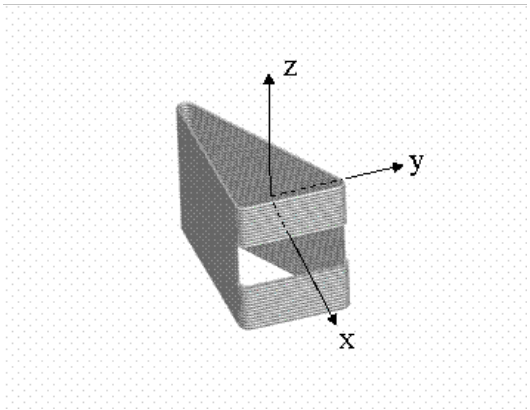

Figure 5: Schematic of a single triangular solenoid with a gap in the face through which the neutron beam passes at right angles. The figure omits the flux return paths which ensure that an intact, finite-length solenoid has the same field as an infinitely long solenoid. In practice, the current carrying wires cannot end on the vertical gap edges and have to be bent above or below the gap (Figure 6).

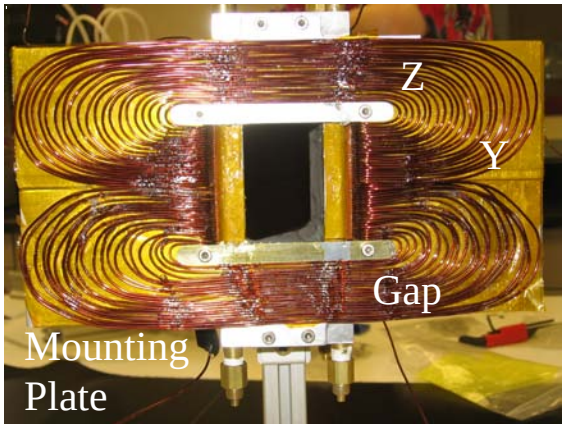

Figure 6: View of triangular Solenoid along the neutron beam.

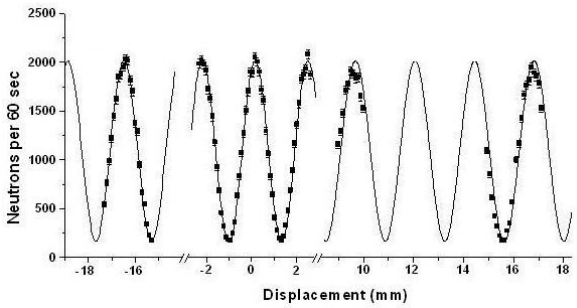

Figure 7: Neutron intensity transmitted through a pair of triangular solenoids as a function of the displacement across the neutron beam (y-direction in Figure 5). The sinusoidal curve was only fitted to the data around zero displacement, but can be seen to fit the data at much larger displacements, demonstrating that the field integral through the triangle-pair varies linearly with displacement in the y direction. Data were obtained at the NCNR [3].

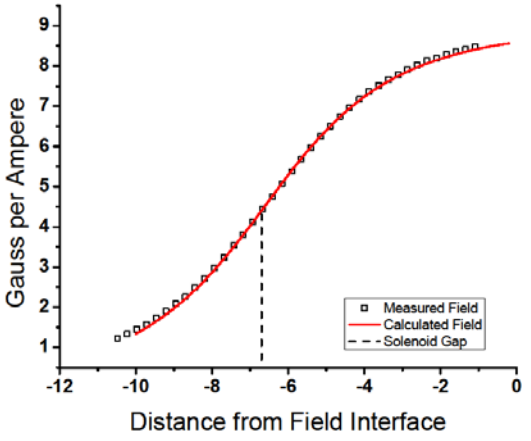

Figure 8: Plot of the measured and simulated magnetic field generated by a triangle pair, versus distance from the interface between two triangular solenoids along the neutron beam-line (x in Figure 5).

the frame is negligible, so all six water pipes in each pair of coils are run in series. The wires folded back from the gaps (Figure 6) are passively cooled via heat sinks on the rear of the mounting plates. The four pairs of triangular solenoids are connected in parallel in the water circuit. The water supply operates at room temperature and runs at sixty psi. This cooling allows us to maintain stable temperature with 16A through the solenoids.

SESAME also requires π and $\pi/2$ flipping devices. Both types of flippers are constructed in a manner similar to the triangular solenoids. The same aluminum wire is wrapped around a rectangular, aluminum frame, which is a simple 1/2" thick shell in this case. The solenoids have a height (parallel to the field direction) of 14.0 cm, a width of 7.0 cm, and extend 7.0 cm along the neutron beamline. They are yoked in the same thickness of mumetal as the triangular solenoids and gaps are produced in the leading faces using the

same custom aluminum piece as was used for the triangular cross section solenoids. Each flipping element is created by the combination of two of these rectangular solenoids; the π flipper uses two parallel coils with windings that produce anti-parallel fields, while the $\pi/2$ flipper is constructed by mounting one rectangular solenoid perpendicular to its neighbor. The non-gapped faces are butted against each other, providing an abrupt magnetic field transition as the neutron passes from one coil to the other. Due to the sudden change in field direction, each neutron is unable to align its spin moment with the new field direction as it passes through this interface, and its spin direction is now changed with respect to the local magnetic field. Since there is no attempt to rotate the neutron's spin adiabatically, this flipper can work for all neutron wavelength without requiring any changes in the solenoid currents. As we only use 7A through these flipping solenoids, they can safely operate with passive cooling.

2.3 Positioning

Triangular solenoids and flippers in the incident neutron beam mount on a Newport x48 rail with a length of 145 cm (Figure 4). This rail is mounted on two adjustable jacks built by Advanced Design Consulting, which have a range of 10 cm and a precision of 5 μm. As the jacks are one meter apart, the incident beamline can be tilted by up to 5.7˚ for reflection of neutrons from horizontal samples.

A sample table with six degrees of freedom is located after the incident flight path on Newport x95 rails, and can be positioned 168 – 180 cm after the exit of the neutron guides. An XYZ stage provides 2-D horizontal adjustability with a range of ±10 cm (precise to 15 μm) and vertical adjustability from 0-10 cm (precise to 1 μm). Beneath the linear stages is a Huber rotation stage with a full 360º of freedom and a precision of 0.005º. Finally, at the top of the sample stage is a 2-axis Huber goniometer with a range of ten degrees in each direction and one millidegree precision. The goniometer rotates about a point 11 cm above its surface. To the extent possible, all of the components in the sample table are non-magnetic.

The downstream Larmor devices, as well as the polarization analyzer and detector, are mounted on an adjustable optic table purchased from Advanced Design Consulting. A square grid of M6 screw holes spaced every 25 mm covers the table and allows any additional apparatus to be mounted. The table has six degrees of freedom. It rests on three jacks with a range of 10 cm and a precision of 5 μm. The front and rear jacks are separated by 105 cm, allowing the table to be tilted by 5.4˚ for liquids reflectometry. Additionally, the table uses motorized sliders to allow it to rotate in the horizontal plane. Each slider has a range of five centimeters in each direction with 4 μm precision. Finally, the entire table can be rotated (with some difficulty) out of the beam by as much as 90˚ to carry out diffraction experiments.

2.4 Detectors

At the exit of the second neutron guide is a low efficiency (0.5%) Helium-3 detector acting as a neutron monitor. The monitor is 75 mm ×25 mm ×19 mm and thus covers the entire guide exit. We collect the data from the monitor in 50 μs bins to obtain time of flight information.

Currently we use a two dimensional scintillating detector [4] produced by Lexitek [5], mounted 368 cm after the exit of the neutron guides. The detector uses a scintillator of ZnS:Ag doped with ^{6}Li. A mirror behind the scintillator, set at 45º, is used to reflect the light to imaging components that are kept out of the beam. After a photon reflects from the

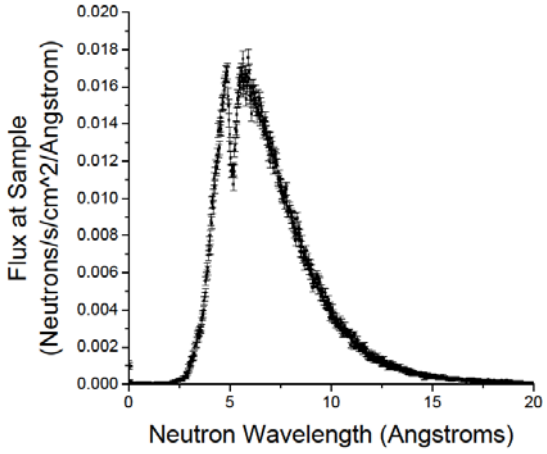

Figure 9: Intensity spectrum of the neutron beam at the sample position in Neutrons cm^{-2} s^{-1}

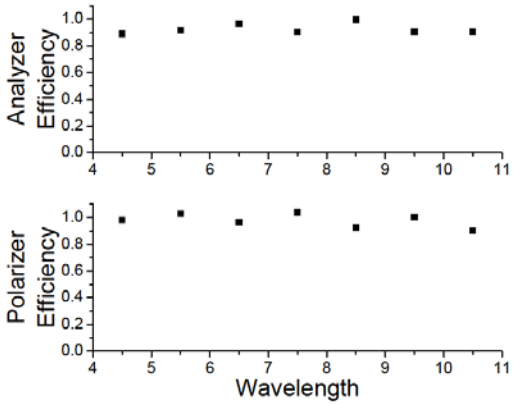

Figure 10: Measured polarizing efficiencies of the polarizing bender and wide angle analyzer.

mirror, it travels to either one of six large photomultiplier tubes (PMTs) or an image intensifier. The output of the image intensifier is read by twenty-one smaller PMTs, each of which is covered by a Gray-coded mask that identifies the light source to within 0.49 mm in the horizontal and vertical directions. The total detector image is 512×512 pixels. To reduce electronic noise, events on the smaller PMTs are corroborated against events on the six larger PMTs, ensuring that the light signal is real. While the detector is capable of 13ns time of flight resolution, we use 250ns time bins, which correspond to 0.1 angstroms in the time of flight.

3. Instrument Characterization

3.1 Neutron Flux

A high efficiency (~100%) ^{3}He pencil detector, measuring 100 mm wide x 25 mm tall and mounted at the sample position, was used to measure the neutron flux. A thin slit, ±1 mm tall and ±10 mm wide, was used to define the beam area and to insure that the beam hit the center of the detector. The LENS proton power-on-target was 2.1 kW during this measurement. The dip in the spectrum at 5.06 Å (Figure 9) is a result of diffraction from the {1 1 1} plane of Si in the bender and has been reported for previous solid-state benders [6]. The total neutron flux integrated over the wavelength range from 4 to 11 Angstroms was 105 Neutrons cm^{-2} s^{-1}. To test the efficiency of the scintillating detector, the pencil detector was removed and the measurement repeated with the scintillating detector. The measured efficiency of the latter was $86 \pm 2\%$ across all wavelengths.

3.2 Flippers

To test their efficiencies, two π flippers were placed between the bender and analyzer and measurements made with the four possible combinations of flipper states. Using these measurements, it is possible to calculate the efficiency of the flippers [7]. In our initial tests, both flippers were more than 95% efficient in the “off” state and slightly less efficient in the “on” state. We are currently working to improve this performance.

3.3 Polarizing Efficiency

Determining the individual polarizing efficiencies of the bender and the wide-angle analyzer required the addition of an m=2 polarizing supermirror at the sample position to decouple the two devices and to provide enough independent measurements to be able to deduce the polarizing efficiencies of individual devices. The polarizing efficiency of the bender and wide angle analyzer are plotted in Figure 10. At the current time, we are investigating improvements to the polarizing efficiency of the bender at long wavelengths through an increase in the strength of the magnetic field applied to it (currently this field is between 0.03T and 0.04T).

4. Acknowledgements

Construction of LENS was supported by the National Science Foundation grants DMR-0220560 and DMR-0320627, the 21st Century Science and Technology fund of Indiana, Indiana University, and the Department of Defense. Operation of LENS is supported by Indiana University. The development of the SESAME method is supported by the U.S. Department of Energy, Office of Basic Energy Sciences, Division of Materials Sciences and Engineering (grant No. DE-FG02-09ER46279).

5. References

1. W. G. Bouwmann, M. van Oossanen, O. Uca, W. H. Kraan and M. T. Rekveldt, *J. Appl. Cryst*. **33** (2000) 767
2. Advanced Design Consulting USA, Inc., 126 Ridge Road, P.O. Box 187, Lansing, NY 14882 USA
3. R Pynn, W. T. Lee, P. Stonaha, V. R. Shah, A. L. Washington, B. J. Kirby, C. F. Majkrzak, and B. B. Maranville, *Rev. Sci Instrum.* **79** (2008) 063901.
4. C. Papaliolios, P. Nisenson, and S. Ebstein. *Appl. Opt.*, **24** (1985) 287
5. Lexitek, Inc., 14 Mica Lane, Wellesley, MA 02481 USA
6. A. Stunault, K. H. Andersen, S. Roux, T. Bigault, K. Ben-Saidane, and H. M. Ronnow, *Physica B*, **385-386** (2006) 1152-1154
7. A. P. Serebrov, A. V. Aldushchenkov, M. S. Lasakov, I. A. Kuznetsov, and I. V. Stepanenko, *Nucl. Instrum. Meth. A*, **357** (1995) 503-510